THE AMERICAN SOCIETY OF MECHANICAL ENGINEERS
345 E. 47th St., New York, N.Y. 10017

98-GT-174

FILM COOLING EFFECTIVENESS AND MASS/HEAT TRANSFER COEFFICIENT DOWNSTREAM OF ONE ROW OF DISCRETE HOLES

R. J. Goldstein, P. Jin and R. L. Olson[1]

Department of Mechanical Engineering
University of Minnesota
Minneapolis, MN 55455, U.S.A.

1 currently at Lockheed Martin Corp., St. Paul, MN

ABSTRACT

A special naphthalene sublimation technique is used to study the film cooling performance downstream of one row of holes of 35° inclination angle with $3d$ hole spacing and relatively small hole length to diameter ratio ($L/d = 6.3$). Both film cooling effectiveness and mass/heat transfer coefficient are determined for blowing rates from 0.5 to 2.0 with density ratio of 1.0. The mass transfer coefficient is measured using pure air film injection, while the film cooling effectiveness is derived from comparison of mass transfer coefficient obtained following injection of naphthalene-vapor-saturated air with that of pure air injection. This technique enables one to obtain detailed local information on film cooling performance. The laterally-averaged and local film cooling effectiveness agree with previous experiments. The difference between mass/heat transfer coefficients and previous heat transfer results indicates that conduction error may play an important role in the earlier heat transfer measurements.

NOMENCLATURE

$\dot{m}$ mass transfer rate per unit area, $=\rho_s(\delta y/\delta\tau)$

$\dot{m}_0$ mass transfer rate per unit area for $\rho_{v,2} = \rho_{v,\infty}$

$\dot{m}_1$ mass transfer rate per unit area for $\rho_{v,2} = \rho_{v,w}$

CA compound angle of injection hole, $=45°$ in present study

d diameter of injection hole, $=6.35mm$ in present study

$D.R.$ density ratio, $=\rho_2/\rho_\infty = 1.0$ in present study

D_{naph} naphthalene vapor diffusivity in air

h heat transfer coefficient

h'_{m0} mass transfer coefficient for $\rho_{v,2} = \rho_{v,\infty}$

h'_{m1} mass transfer coefficient for $\rho_{v,2} = \rho_{v,w}$

$\overline{h}$ lateral-average(over z) of h

h_m impermeable wall mass transfer coefficient

h_o heat transfer coefficient without injection

h_{mo} mass transfer coefficient without injection

I momentum ratio, $=(\rho_2 U_2^2)/(\rho_\infty U_\infty^2)$

IA inclination angle of injection hole, $=35°$ in present study

L length of injection hole

M blowing rate, $=(\rho_2 U_2)/(\rho_\infty U_\infty)$

Re_d Reynolds number based on U_∞ and d, $=\rho U_\infty d/\mu$

s space between the injection holes, $=3d$ in present study

Sc Schmidt number, $=\mu/\rho D_{naph}$, ≈ 2.29 in present study

Sh'_0 Sherwood number for $\rho_{v,2} = \rho_{v,\infty}$

$\overline{Sh'_0}$ lateral-average(over z) of Sh'_0

Sh'_1 Sherwood number for $\rho_{v,2} = \rho_{v,w}$

Sh_o Sherwood number based on h_{mo}, $=h_{mo}d/D_{naph}$

t thickness of the injection plate

Tu free stream turbulence intensity, $\approx 0.54\%$ in present study

U_2 secondary flow velocity

Presented at the International Gas Turbine & Aeroengine Congress & Exhibition
Stockholm, Sweden — June 2–June 5, 1998
This paper has been accepted for publication in the Transactions of the ASME
Discussion of it will be accepted at ASME Headquarters until September 30, 1998

U_∞ mainstream velocity

$V.R.$ velocity ratio, $=U_2/U_\infty$

x streamwise distance from the center of injection hole

y distance normal to film cooling wall

z spanwise distance from the center of the injection hole

Greek Symbols

$\delta\tau$ time interval for naphthalene sublimation in forced convection

δ^* boundary layer displacement thickness

δy local naphthalene sublimation depth in forced convection

η_{iw} impermeable wall film cooling effectiveness

$\overline{\eta_{iw}}$ laterally-averaged impermeable wall film cooling effectiveness

ρ_2 secondary flow density

ρ_s density of solid naphthalene

ρ_∞ mainstream density

$\rho_{v,2}$ naphthalene vapor density in the secondary flow

$\rho_{v,\infty}$ naphthalene vapor density in the mainstream

$\rho_{v,iw}$ naphthalene vapor density at the impermeable wall

$\rho_{v,w}$ naphthalene vapor density at the wall

INTRODUCTION

To increase the efficiency of gas turbine systems, the inlet temperatures of first stage turbine have been raised significantly over the last decade. One of the consequences of this is the potential failure of components in the turbine section due to large thermal stresses. As the inlet temperatures increases, material limits such as the creep and failure of turbine components is of great concern. Film cooling is one of the cooling schemes being used to reduce these problems. Air is bypassed from the compressor (often after the last stage) into the high performance blade or vane where it is used for internal cooling and then is ejected through the blade surface into the external boundary layer to reduce the temperature in the boundary layer and protect the surface over which the hot combustion gas flows.

Due to manufacturing and stress-related reasons, discrete-hole film cooling is preferred rather than slot injection film cooling. The discrete-hole geometry leads to three dimensional flow and temperature fields downstream of injection. Jet liftoff, high turbulence intensity in the shear layer, and double counter-rotating vortices are important features of film cooling cited by many researchers.

The performance of film cooling is usually characterized by two figures of merit: the adiabatic wall effectiveness and heat transfer coefficient. Various geometrical and fluid dynamics parameters can affect the performance of discrete hole film cooling. To name a few, hole spacing (s/d), length of hole (L/d), shape of hole, inclination angle (IA), compound angle (CA), surface curvature, and smoothness of the surface are common geometrical factors while the fluid dynamics parameters include blowing rate (M), momentum flux ratio (I), density ratio ($D.R.$), velocity ratio ($V.R.$) free-stream turbulence intensity (Tu) and length scale, and mainstream pressure gradient.

Many studies have been conducted on the performance of discrete hole film cooling. While in most studies heat transfer measurements were made (eg. Eriksen and Goldstein (1974), Sinha et al. (1990)), mass transfer and the heat/mass transfer analogy method were studied by Pedersen et al. (1977) and Foster and Lampard (1980). In most studies, the detailed local values of film cooling effectiveness and heat transfer coefficient were not available due to the measurement methodology and averaged values were usually presented. Wall conduction errors in heat transfer experiments are often problematic. On the other hand, the modern development of gas turbine technology demands detailed information on film cooling effectiveness and heat transfer coefficient, especially immediately downstream of injection holes. In this study, the naphthalene sublimation technique is used to obtain detailed local information of film cooling effectiveness and mass/heat transfer coefficient downstream of one row of inclined holes.

Recently, the effects of hole geometry on the fluid dynamics and film cooling performance have been actively investigated by many researchers. Sinha et al. (1990) studied the adiabatic effectiveness downstream of one row of inclined holes with short length ($L/d = 1.75$) under various density ratios and blowing rates. They showed that short injection-hole length can cause early jet detachment at a small momentum flux ratio. In heat transfer measurements, Sen et al. (1996) and Schmidt et al. (1996) investigated the adiabatic wall effectiveness and heat transfer coefficient using a single row of inclined holes with different shapes, compound angles and a hole length of $4d$. They found the geometry could influence the film cooling performance greatly. Ekkad et al. (1997b) and Ekkad et al. (1997a) presented film cooling effectiveness and heat transfer coefficient distributions over a flat surface with one row of inclined holes for different compound angle and density ratios at an elevated free stream turbulence intensity ($Tu = 8.5\%$) using a transient liquid crystal technique proposed by Vendula and Metzger (1991), which can determine local effectiveness and heat transfer coefficient distribution simultaneously. A hole length to diameter ratio (L/d) of 4.6 was used in their study.

In the present study, one row of discrete film cooling holes on a flat plate with inclination angle of 35° and a length to diameter ratio of 6.3 is investigated using naphthalene sublimation technique and mass/heat transfer analogy, by which the detailed local information of effectiveness and mass transfer coefficient can be attained. The blowing rate varies from 0.5 to 2.0 with the density ratio of 1.0.

EXPERIMENTAL METHOD AND NAPHTHALENE SUBLIMATION TECHNIQUE

Eckert (1984) analyzed two approaches used in film cooling experiments. The first uses the adiabatic wall temperature (effectiveness) and a heat transfer coefficient only dependent on the fluid mechanics, which is arguably the most prevalent method used in research and industry. The second approach uses a dimensionless temperature and hence a heat transfer coefficient varying linearly with the dimensionless temperature. Both methods utilize the linear energy equation under the condition of constant fluid properties to enable the superposition of temperature field. Eckert (1984) showed the results of the two approaches are convertible under condition of small temperature gradients on the film cooled wall.

The naphthalene sublimation method and the heat/mass transfer analogy were reviewed by Goldstein and Cho (1995); the advantages as well as the measurement technique were analyzed and compared to heat transfer results. Cho and Goldstein (1995a) and Cho and Goldstein (1995b) measured film cooling effectiveness and mass/heat transfer coefficient for full coverage film cooling on a flat plate using the naphthalene sublimation.

In summary, the naphthalene sublimation technique can be used to determine the convective component of heat transfer with the absence of wall conduction and radiation errors. A mass transfer problem can be converted to a heat transfer problem under the same boundary conditions by mass/heat transfer analogy. Following Cho and Goldstein (1995a), using the naphthalene sublimation technique and the isothermal conditions, the mass/heat transfer coefficient for film cooling on a flat plate downstream of one row of holes can be obtained by measuring the mass transfer coefficient of the naphthalene wall with pure air injection,

$$h_m = h'_{m0} = \frac{\dot{m}_0}{\rho_{v,w} - \rho_{v,\infty}} \quad \text{when } \rho_{v,2} = \rho_{v,\infty}$$
$$= \frac{\dot{m}_0}{\rho_{v,w}} \quad \text{since } \rho_{v,\infty} = 0 \text{ in present study} \tag{1}$$

The dimensionless mass transfer coefficient defined as Sherwood number is used and often normalized by the mass transfer coefficient on the same flat plate without injection of secondary flow to cancel the effects of unheated starting length and Sherwood (Prandtl) number, making it comparable to the normalized heat transfer coefficient (h/h_o).

$$\frac{Sh'_0}{Sh_o} = \frac{h_m}{h_{mo}} = \frac{h'_{m0}}{h_{mo}} \tag{2}$$

The isothermal (iso-concentration) wall film cooling effectiveness, which is shown by Eckert (1984) to be convertible to the adiabatic (impermeable) wall effectiveness, can be attained by comparing the mass transfer coefficient measured with injection of naphthalene-vapor-saturated air at the ambient temperature with the mass transfer coefficient measured with pure air injection,

$$h'_{m1} = \frac{\dot{m}_1}{\rho_{v,w} - \rho_{v,\infty}} \quad \text{when } \rho_{v,2} = \rho_{v,w}$$
$$= \frac{\dot{m}_1}{\rho_{v,w}} \quad \text{since } \rho_{v,\infty} = 0 \text{ in present study} \tag{3}$$

$$\eta_{iw} = \frac{\rho_{v,iw} - \rho_{v,\infty}}{\rho_{v,2} - \rho_{v,\infty}} = 1 - \frac{h'_{m1}}{h'_{m0}} = 1 - \frac{Sh'_1}{Sh'_0} \tag{4}$$

The above method is used in the data reduction of the present investigation to get the effectiveness.

EXPERIMENTAL FACILITY AND QUALIFICATION TEST

A large open cycle, suction type wind tunnel in the Heat Transfer Laboratory at the University of Minnesota is used to supply the mainstream for the film cooling test. Flow to the 2500*mm* long, 305.0*mm* high and 610.0mm wide test section is preceded by a flow straightener and a 15 : 1 area contraction. The side and top walls of the test section are made of Plexiglas. The film cooling injection plate perforated with one row of holes and naphthalene test plate are installed in the bottom wall of the test section. The plan view of the test section is shown in Fig.1. A 1.0*mm* diameter trip followed by a 25.4*mm* strip of sandpaper

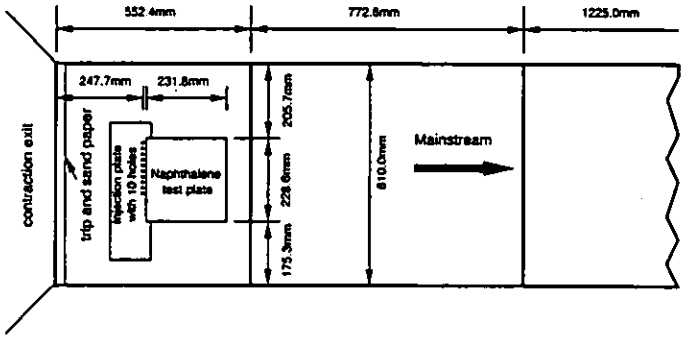

Figure 1: Planview of test section

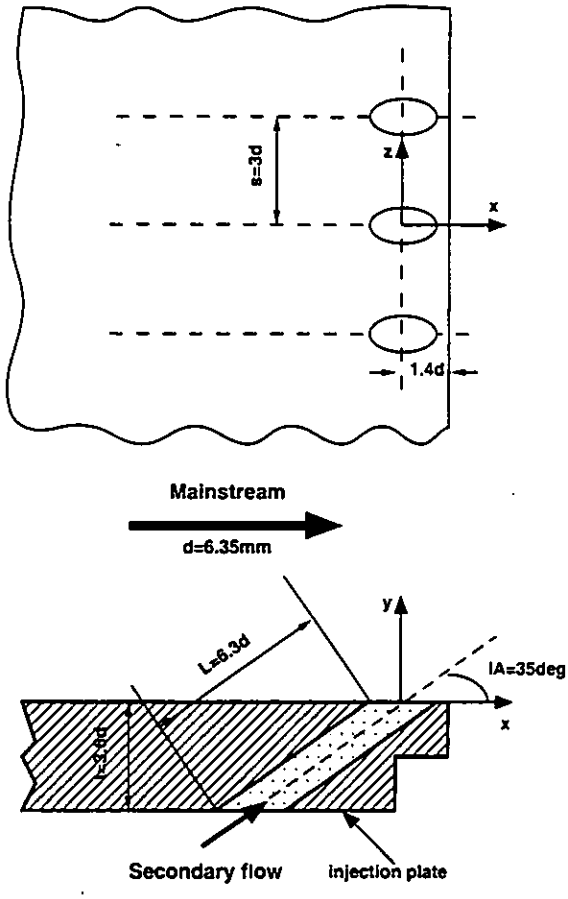

Figure 2: Film cooling hole geometry

is set up at the exit of the contraction to trip and smooth the turbulent boundary layer developed on the flat wall. The center of the holes is 247.7*mm* downstream of the trip.

The details of the injection hole are shown in Fig.2. The one row of holes of 6.35*mm* diameter is inclined at 35° to the direction of mainstream with a 3*d* hole spacing. The injection plate is 22.9*mm* thick and made of aluminum, providing a hole length of 6.3*d*. The coordinate directions are also shown in the same figure. In many previous studies, the origin of the coordinate system is often placed at the downstream tip of the hole. It is not a major issue when dealing with straight holes without compound angle. However, it is more appropriate to put the origin of the coordinate at the center of the injection holes when compound angle

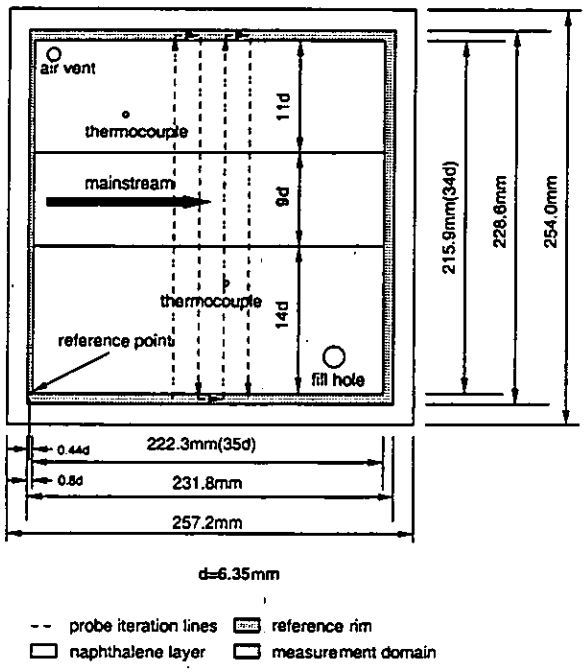

Figure 3: Naphthalene sublimation test plate

geometry is used. To comply with later investigations of compound angle injection, the origin of the coordinates is placed at the center of hole in this study. Results from other studies are corrected for this definition of x.

The aluminum naphthalene test plate is located immediately downstream of the holes to facilitate the investigation of film cooling performance near the hole. Fig.3 shows the geometry of the naphthalene plate. The naphthalene casting layer is $35d$ long, $34d$ wide and $2.54mm$ thick, of which only a $9d$ wide strip around the centerline of the test section (covering 3 holes) is used to measure the mass transfer coefficient. Two thermocouples are placed from the back up near the surface of the naphthalene layer to monitor the surface temperature. The fill hole and air vent are used in naphthalene casting. The reference point and aluminum rim around the naphthalene layer are used as the references in the naphthalene sublimation profile measurement.

Fig.4 shows the secondary air injection system. Compressed air from the building supply passes through a $50.8mm$ diameter piping system equipped with valve, flow regulating orifice, tape heater and thermocouple which provide control of the secondary air flow rate and temperature. At the end of the pipe, the secondary air goes into a plenum chamber $133.35mm$ wide, $414.7mm$ long and $850.9mm$ high. The air first passes through a screen at the inlet of the plenum and then a flat screen for pure air injection or two layers of naphthalene powder in the naphthalene-vapor- saturated air injection case. Then the flow goes along the plenum passage and out through the injection holes into the mainstream. Thermocouples are installed to monitor the temperature of the flow in the mainstream, plenum and surrounding air.

The T type thermocouples and orifice meter used in the experiment was previously calibrated by Cho (1992). The thermocouples are integrated with a GPIB board enabled Linux workstation to facilitate the temperature measurement of the film cooling system. The total pressure is measured with a total pressure tube located $300mm$ downstream of the holes and a static pressure tap is $20mm$ upstream of the total pressure tube. Both of these are connected to a micro-manometer with a reading precision of $0.01mmH_2O$ to give the mainstream velocity. The secondary air flow is determined by measuring the pressure drop across the calibrated orifice in the pipe with a manometer system and is adjusted by the valve. The depth change of the naphthalene layer during the film cooling test is measured with an automated XY-table surface profile measuring system developed in the Heat Transfer Laboratory at the University of Minnesota. The details of the system and calibration procedure can be found in Cho (1992) and Olson (1996).

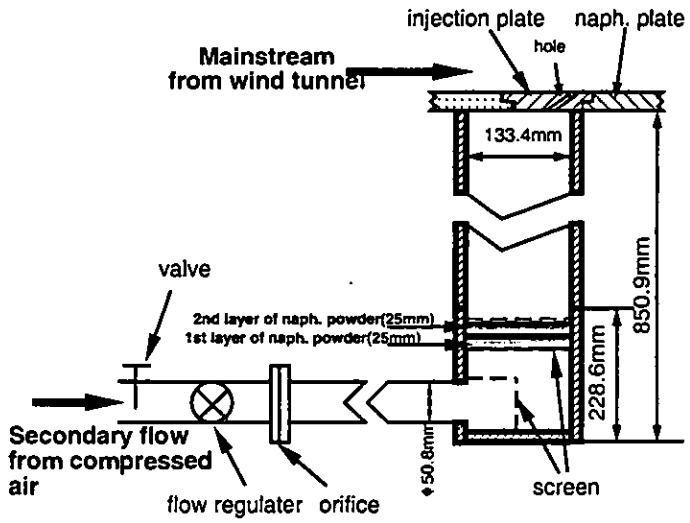

Figure 4: Secondary flow injection system

The uncertainty in naphthalene wall temperature measurement is 0.09% with 95% confidence level. The uncertainty in mainstream and secondary flow velocity is 1.4% and 2.5% respectively. The uncertainty in blowing rate is 2.7% while in the naphthalene sublimation depth change it is within 0.80%, which includes the error of repositioning. The uncertainty in mass transfer coefficient and Sherwood number are 5.4% and 7.4% at 95% confidence level respectively. The relative uncertainty in effectiveness is local-effectiveness dependent in this method and is 6.2% for higher effectiveness of 0.5 and less than 27% for low effectiveness of 0.2. The relaiively large error in Sherwood number is mainly caused by the uncertainty in property parameters of naphthalene. The naphthalene loss due to natural convection is estimated and included in the above uncertainty analysis. The experimental procedure is described by Olson (1996) in detail.

The turbulent boundary layer established downstream of the trip without secondary air injection is described in Table 1. The mass transfer Stanton numbers downstream of (taped) holes without injection are measured and compared with heat transfer Stanton numbers with unheated starting length calculated from empirical equations. Good agreement is obtained. For a typical sublimation depth of $50\mu m$, the effect of thinner naphthalene wall on boundary layer thickness (of order of $10mm$) is neglected. Since the pressure of saturated naphthalene vapor is four orders of magnitude less than the atmospheric pressure, the fluid properties for saturated-naphthalene-vapor injection are considered to be constant. Thus, the density ratio is essentially unity. The saturation of naphthalene vapor in the air is assured by comparing results for two different thicknesses of the naphthalene layers used to add vapor to the injected flow and is confirmed by the repeatability of the results. The repeatability of mass transfer coefficient for both pure air film injection

Table 1: Film cooling geometry and operating conditions

$d(mm)$	s/d	L/d	IA(deg)	CA(deg)	x/d range
6.35	3	6.3	35	0	2-36
$U_\infty(m/s)$	$Tu(\%)$	δ^*/d	Re_d	M	D.R.
15.7	0.54	0.238	6300	0.5-2.0	1.0

and naphthalene-vapor-saturated air injection is demonstrated in Olson (1996) and considered in the experiments uncertainty analysis.

EXPERIMENTAL RESULTS AND DISCUSSION

Film Cooling Effectiveness

The laterally-averaged film cooling effectiveness is compared with previous results for blowing rates of 0.5, 1.0, and 2.0 in Fig.5. General agreement with heat transfer data of Goldstein et al. (1969) and mass transfer data of Pedersen et al. (1977) can be found for the three blowing rates. The effect of the relatively short hole ($L/d = 6.3$) used in the present case on the effectiveness is not obvious for low and high blowing rates of 0.5 and 2.0 when compared with the results of long tubes used in the experiments of Pedersen et al. (1977) and Goldstein et al. (1969). For the moderate blowing rate of 1.0, the relatively low effectiveness immediately downstream of the injection holes is apparently due to the short hole effect. At low blowing rate the secondary flow velocity distribution is relatively uniform and similar to that of the long-tube case while the high momentum flux caused liftoff of the secondary flow which strongly affects the film cooling at the high blowing rate. At a blowing rate of 1.0 , however, the non-uniformity of velocity of secondary flow due to the jetting effect of short holes apparently increases the possibility of liftoff and causes low effectiveness near the hole. The much higher film cooling effectiveness $20d$ downstream of the holes at a blowing rate of 2.0 may be due to the increased turbulent mixing induced by strong interaction of the mainstream with the injected jets.

The low effectiveness Sinha et al. (1990) found at $M = 0.5$ may be due to the much shorter hole length to diameter ratio ($L/d = 1.75$) used. For the case of Ekkad et al. (1997b), the high free stream turbulence intensity of 8.5% causes strong mixing of coolant and mainstream, hence the even lower film cooling effectiveness at low blowing rate. With an increase of blowing rate, the turbulent mixing decelerates the liftoff of secondary flow and provides better coverage of film on the film cooled wall. Therefore, the effectiveness is relatively high in the near-hole region and more uniform further downstream with large Tu.

The local film cooling effectiveness $11d$ downstream of injection holes for blowing rates of 0.5 and 1.0 is shown in Fig.6. The general agreement with data of Pedersen et al. (1977) and Goldstein et al. (1969) can be observed. Thus, it seems at this position, not very close to the injection holes, the relatively short holes used in the present study provides effectiveness similar to that found with long holes. The results of Sinha et al. (1990), also shown for $M = 0.5$, are consistently lower than other results apparently owing to the much smaller hole length to diameter ratio used.

Contour plots of effectiveness for $M = 0.5$, 1.0 and 2.0 are provided in Fig.7 respecively. At $M = 0.5$, the effectiveness attains its highest value of 0.4 along the centerline of the holes near $x/d = 3$. The low effectiveness region midway between the holes is narrow compared with the width ($2d$) of the relatively high effectiveness area ($\eta_{iw} \geq 0.1$) downstream of holes. As the blowing rate increases to 1.0, the peak of effectiveness is about 0.2 along the centerline of the hole at $x/d = 6$ while the low effectiveness region between the holes grows wide and the relatively high effectiveness area narrows to about $1d$. At blowing rate of 2.0, the above mentioned two regions merge by $x/d = 16$

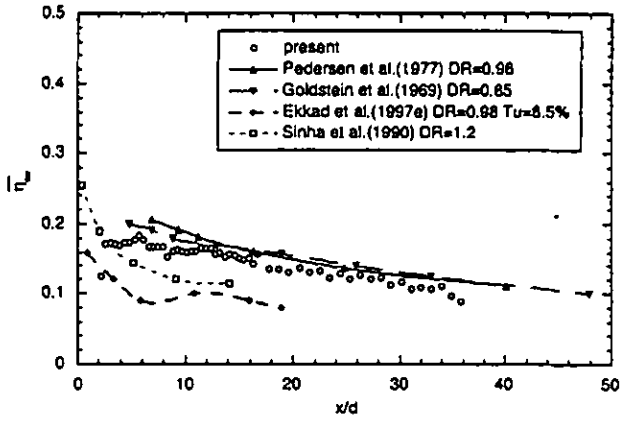

(a) M=0.5

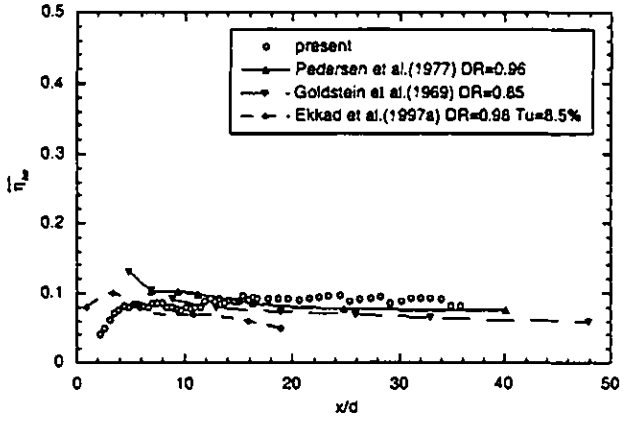

(b) M=1.0

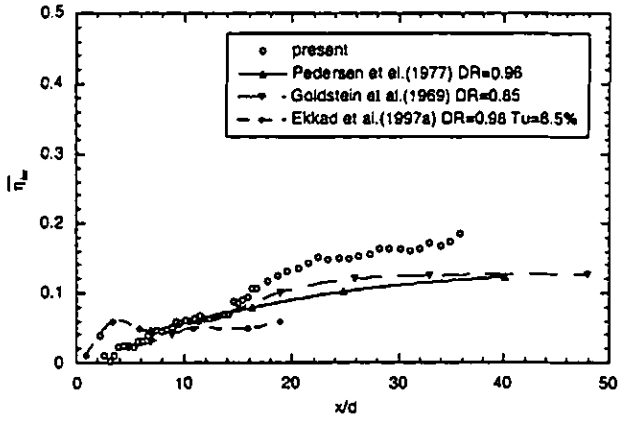

(c) M=2.0

Figure 5: Comparison of $\overline{\eta_{iw}}$

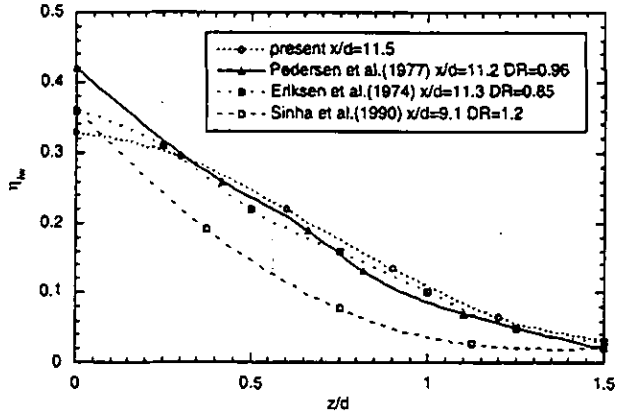

(a) M=0.5

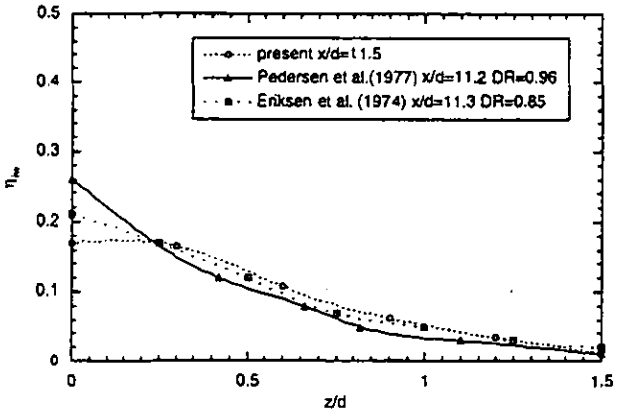

(b) M=1.0

Figure 6: Comparison of local η_{iw}

and form a uniform and moderate effectiveness region ($\eta_{iw} \geq 0.1$) after $x/d = 18$. These contour plots indicate that with an increase of blowing rate from 0.5 to 1.0, the coverage of the secondary flow decreases due to the liftoff effect. High effectiveness occurs when the secondary flow touches down on the wall. Further increasing blowing rate to 2.0, the increased interaction between the mainstream and the secondary flow spreads the secondary flow to midway between the holes and flattens the distribution of effectiveness in downstream areas.

Mass/Heat Transfer Coefficient

Comparisons of laterally-averaged and normalized Sherwood number and heat transfer coefficient are plotted for $M = 0.5$, 1.0 and 2.0 in Fig.8 respectively. The agreement with experiment of Eriksen and Goldstein (1974) becomes better at the near-hole region for blowing rate of 2.0 while the data appear collapsed to one curve further downstream at the low blowing rate of 0.5 and 1.0. The difference among the data can't be explained by the effect of hole length to diameter ratio because the results of Sen et al. (1996) and Ekkad et al. (1997a) are for the short hole geometry while the data from Eriksen and Goldstein (1974) are for long-tube injection. The effect of Reynolds number may not be a large factor

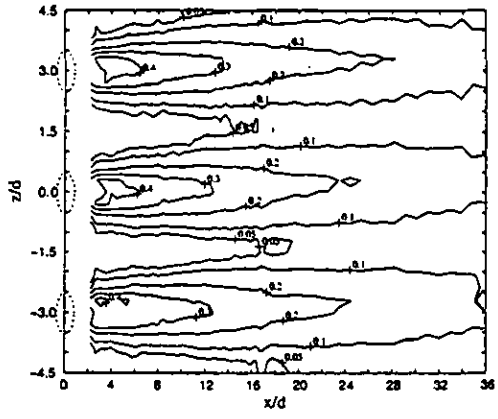

(a) M=0.5

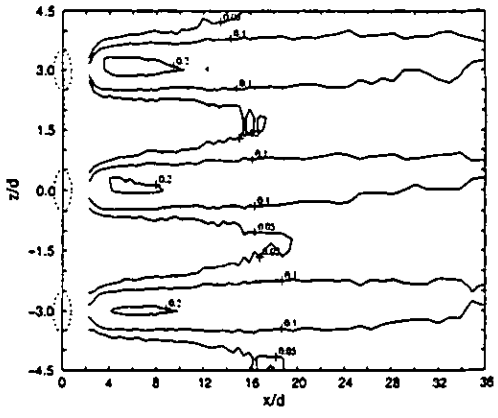

(b) M=1.0

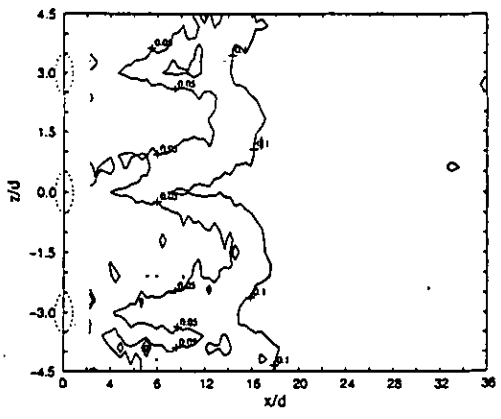

(c) M=2.0

Figure 7: Local η_{iw} contour

for these experimental results since the Reynolds number ranges from 6000 to 22000. The different trend of data from Ekkad et al. (1997a) at

blowing rate of 2.0 may be caused by the high free stream turbulence level.

The comparisons of local normalized Sherwood number and heat transfer coefficient in Fig.9 provides some insight. The present study and that of Goldstein and Taylor (1982) both used naphthalene sublimation though the latter used long tubes while the data of Eriksen and Goldstein (1974) and Sen et al. (1996) were from heat transfer measurements. The results from the different naphthalene sublimation measurements are relatively close. The variation of heat transfer results in the lateral direction (z) are small compared with that in the present study, especially for higher blowing rates. This suggests that heat conduction errors may play an important role in the heat transfer measurement.

Contour plots for normalized Sherwood number are shown in Fig.10 for blowing rates of 0.5, 1.0 and 2.0 respectively. Regions of high and low mass transfer are shown in Fig.11. Two regions of high mass transfer immediately downstream of the injection holes can be observed. At the low blowing rate of 0.5, the secondary flow remains attached to the naphthalene wall due to its low momentum flux ratio to the mainstream. Thus, the mass transfer rate at the centerline of the holes is even lower than without injection since the boundary layer becomes thicker. The area midway between the holes is not covered by the injected film so that the mass transfer rate remains almost the same as the case without injection. Immediately downstream of the holes, the mass transfer rate is higher at the edge of the secondary flow probably due to the interaction between the mainstream and secondary flow. This high mass transfer region is similar to region "D" described in Goldstein and Taylor (1982), resulting from large shear stresses and eddies created by mainstream and secondary flow interaction.

At the higher blowing rates of 1.0 and 2.0, the secondary flow lifts off from the wall. Due to the blockage of mainstream by the secondary flow liftoff, the mainstream penetrates underneath the secondary flow by induced pressure deficit and sweeps the wall under the injected flow heavily. Therefore, the mass transfer rate immediately downstream of the hole increases drastically at these blowing rates and forms a high mass transfer region similar to region "E" in Goldstein and Taylor (1982). The peak of the mass transfer coefficient stays at about $x/d = 4$ while this high mass transfer region, due to mainstream sweeping, extends further downstream for higher blowing rates. The interaction between the mainstream and secondary flow is also greater at the edge of the secondary flow, extending the high mass transfer area observed at blowing rate of 0.5, but this effect is only secondary to the sweeping of the mainstream under the injected flow. The mass transfer coefficients further downstream and midway between the holes are also higher than that at the centerline of holes for the blowing rates. This is induced by the spreading and merging of two neighboring jets, and the interacting vortex structures, midway between the holes, and the increasing boundary layer thickness due to the re-attached flow along the centerline.

From these contour plots, we can see that the secondary flow from each hole remains separate until $x/d = 34$ for blowing rate of 0.5. At the blowing rate of 1.0, the secondary flow merges at about $x/d = 12$. For the highest blowing rate of 2.0, it seems the secondary flow spreads and merges immediately after injection due to the strong interaction of the neighboring jets with each other and with the mainstream.

CONCLUSION

In the present study, the naphthalene sublimation technique and the heat/mass transfer analogy are used to measure the film cooling performance for one row of holes with 35° inclination angle. The mass

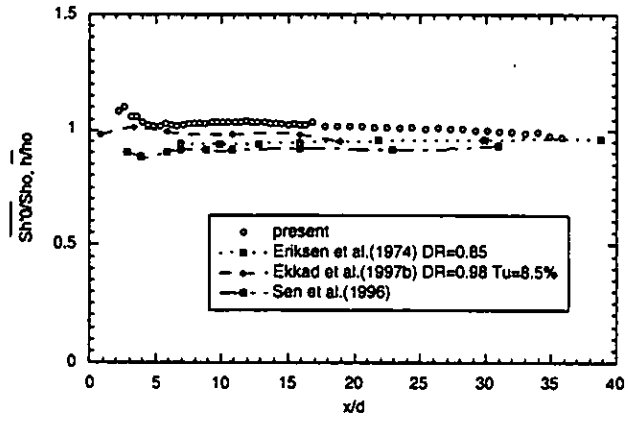

(a) M=0.5

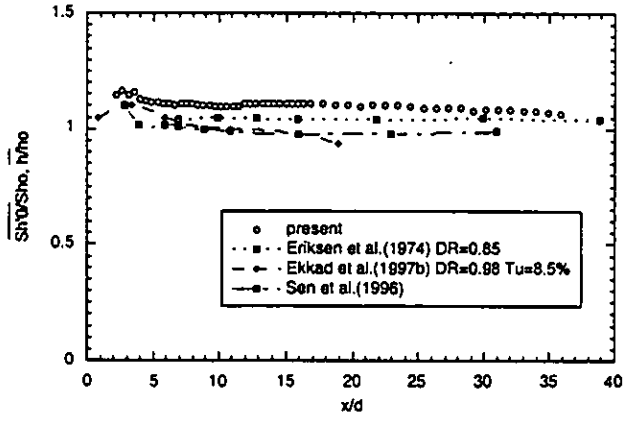

(b) M=1.0

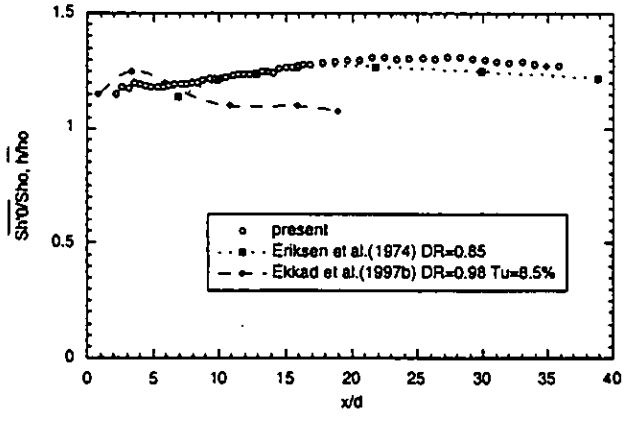

(c) M=2.0

Figure 8: Comparison of $\overline{Sh_0'}/Sh_o$

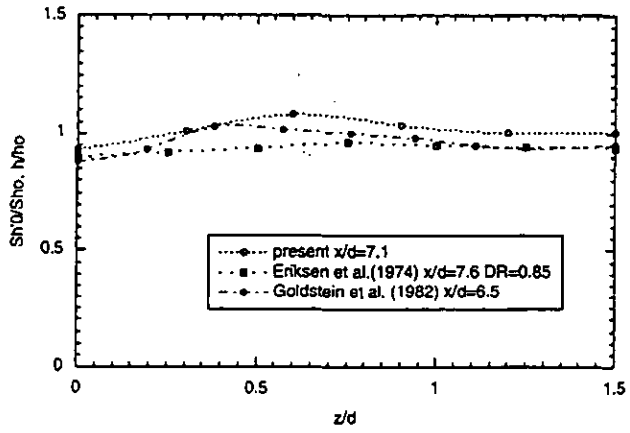

(a) M=0.5

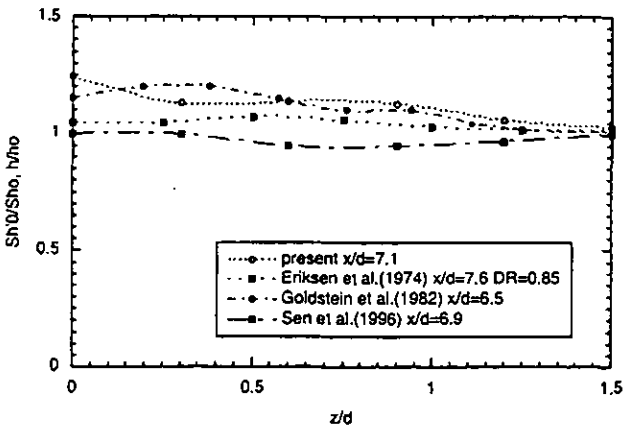

(b) M=1.0

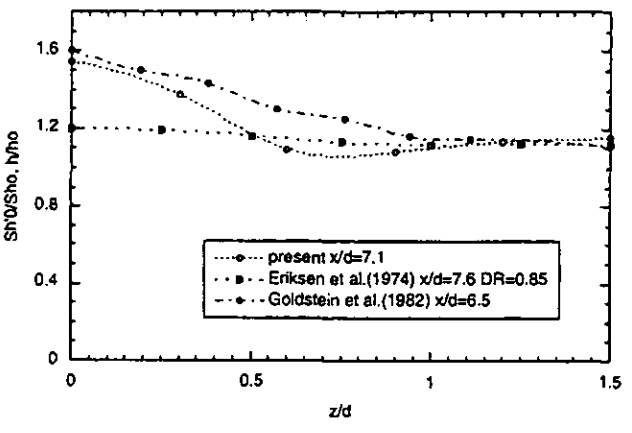

(c) M=2.0

Figure 9: Comparison of local Sh'_0/Sh_o

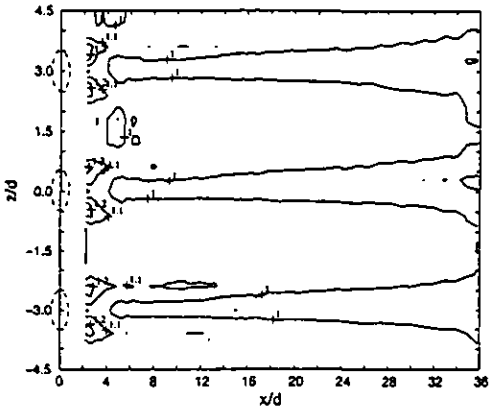

(a) M=0.5

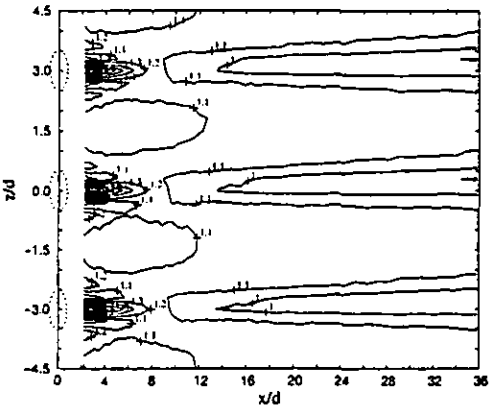

(b) M=1.0

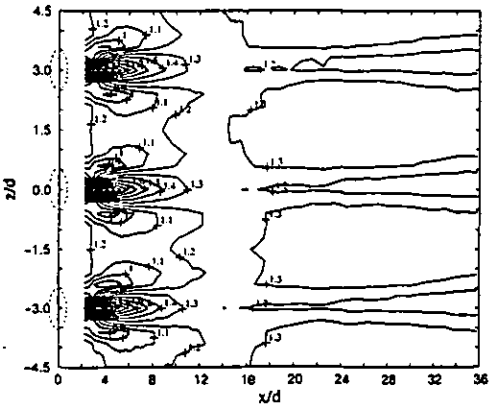

(c) M=2.0

Figure 10: Local Sh'_0/Sh_o contour

transfer coefficient is measured using pure air film injection while the film cooling effectiveness is derived from comparison of mass transfer

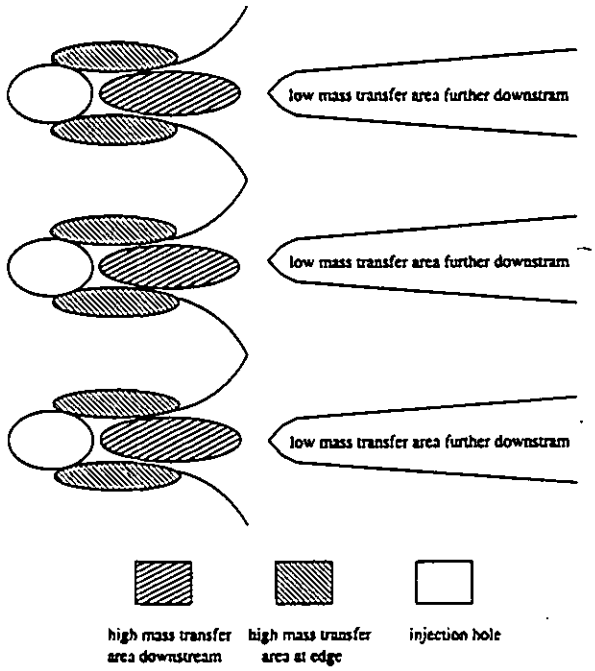

Figure 11: Regions of high and low mass transfer

coefficients obtained following injection of naphthalene-vapor-saturated air with that of pure-air. The following conclusions can be made:

1. the local and the laterally-averaged film cooling effectiveness generally agree with previous results at blowing ratio of 0.5 and 1.0. The relatively short injection hole configuration used provides an effectiveness similar to that found with long injection holes at similar blowing rates.

2. the local and the laterally-averaged mass transfer coefficients obtained in the present study do not agree as well with previous heat transfer results perhaps due to conduction effects in the region of large temperature gradient in the heat transfer measurements.

3. the naphthalene sublimation technique and the heat/mass transfer analogy used in the present experiment can be used to obtain both detailed local and averaged information on film cooling performance.

REFERENCES

Cho, H. H., 1992. *Experimental Study of Flow and Local Mass/Heat Transfer from Single Short Cylinders and Arrays of Short Pin-Fins in Crossflow.* Ph.D. Thesis, University of Minnesota, Minneapolis, Minnesota.

Cho, H. H. and Goldstein, R. J., 1995a. "Heat(Mass) Transfer and Film Cooling Effectiveness with Injection through Discrete Holes. 1. Within Holes and on the Back Surface." *ASME Journal of Turbomachinery*, vol. 117, pp. 440–450.

Cho, H. H. and Goldstein, R. J., 1995b. "Heat(Mass) Transfer and Film Cooling Effectiveness with Injection through Discrete Holes. 2. On the Exposed Surface." *ASME Journal of Turbomachinery*, vol. 117, pp. 451–460.

Eckert, E. R. G., 1984. "Analysis of Film Cooling and Full-Coverage Film Cooling of Gas Turbine Blades." *ASME Journal of Engineering for Gas Turbine and Power*, vol. 106, pp. 206–213.

Ekkad, S. V., Zapata, D., and Han, J.-C., 1997a. "Film Effectiveness over a Flat Surface with Air and CO_2 Injection through Compound Angle Holes Using a Transient Liquid Crystal Image Method." *ASME Journal of Turbomachinery*, vol. 119, pp. 587–593.

Ekkad, S. V., Zapata, D., and Han, J.-C., 1997b. "Heat Transfer Coefficient over a Flat Surface with Air and CO_2 Injection through Compound Angle holes using a Transient Liquid Crystal Image Method." *ASME Journal of Turbomachinery*, vol. 119, pp. 580–586.

Eriksen, V. L. and Goldstein, R. J., 1974. "Heat Transfer and Film Cooling Following Injection Through Inclined Circular Tubes." *ASME Journal of Heat Transfer*, vol. 96, pp. 239–245.

Foster, N. W. and Lampard, D., 1980. "The Flow and Film Cooling Effectiveness Following Injection through a Row of Holes." *ASME Journal of Engineering for Power*, vol. 102, pp. 584–588.

Goldstein, R. J. and Cho, H. H., 1995. "A Review of Mass Transfer Measurements Using Naphthalene Sublimation." *Experimental Thermal and Fluid Science*, vol. 8, pp. 416–434.

Goldstein, R. J., Eckert, E. R. G., Eriksen, V. L., and Ramsey, J. W., 1969. "NASA Contract No. NAS 3-7904, Film Cooling Following Injection through Inclined Circular Tubes."

Goldstein, R. J. and Taylor, J. R., 1982. "Mass Transfer in the Neighborhood of Jets Entering Crossflow." *ASME Journal of Heat Transfer*, vol. 104, pp. 715–721.

Olson, R. L., 1996. *Film Cooling Effectiveness and Heat(Mass) Transfer Coefficient for a Sigle Row of Discret Film Cooling Holes.* Master's Thesis, University of Minnesota, Minneapolis, Minnesota.

Pedersen, D. R., Eckert, E. R. G., and Goldstein, R. J., 1977. "Film Cooling With Large Density Differences Between the Mainstream and the Secondary Fluid Measured by the Heat-Mass Transfer Anglogy." *ASME Journal of Heat Transfer*, vol. 99, pp. 620–627.

Schmidt, D. L., Sen, B., and Bogard, D. G., 1996. "Film Cooling with Compound Angle Holes-Adiabatic Effectiveness." *ASME Journal of Turbomachinery*, vol. 118, pp. 807–813.

Sen, B., Schmidt, D. L., and Bogard, D. G., 1996. "Film Cooling with Compound Angle Holes-Heat Transfer." *ASME Journal of Turbomachinery*, vol. 118, pp. 800–806.

Sinha, A. K., Bogard, D. G., and Crawford, M. E., 1990. "Film Cooling Effectiveness Downstream of a Single Row of Holes with Variable Density Ratio." *ASME paper 90-GT-43.*

Vendula, R. J. and Metzger, D. E., 1991. "A Method for the Simultaneous Determination of Local Effectivness and Heat Transfer Distributions in Three-Temperature Convection Situations." *ASME paper 91-GT-345.*